JACS
JOURNAL OF THE AMERICAN CHEMICAL SOCIETY

Subscriber access provided by ISTANBUL TEKNIK UNIV

Article

NMR Identification of Transient Complexes Critical to Adenylate Kinase Catalysis

Jrgen dn, and Magnus Wolf-Watz

J. Am. Chem. Soc., **2007**, 129 (45), 14003-14012• DOI: 10.1021/ja075055g • Publication Date (Web): 13 October 2007

Downloaded from http://pubs.acs.org on February 14, 2009

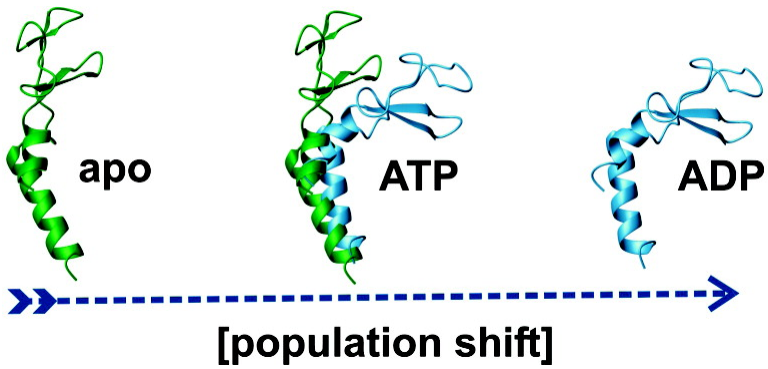

More About This Article

Additional resources and features associated with this article are available within the HTML version:

- Supporting Information
- Links to the 2 articles that cite this article, as of the time of this article download
- Access to high resolution figures
- Links to articles and content related to this article
- Copyright permission to reproduce figures and/or text from this article

View the Full Text HTML

ACS Publications
High quality. High impact.

Journal of the American Chemical Society is published by the American Chemical Society. 1155 Sixteenth Street N.W., Washington, DC 20036

J|A|C|S
ARTICLES
Published on Web 10/13/2007

NMR Identification of Transient Complexes Critical to Adenylate Kinase Catalysis

Jörgen Ådén and Magnus Wolf-Watz*

Contribution from the Department of Chemistry, University of Umeå, SE-901 87 Umeå, Sweden

Received July 9, 2007; E-mail: magnus.wolf-watz@chem.umu.se

Abstract: A fundamental question in protein chemistry is how the native energy landscape of enzymes enables efficient catalysis of chemical reactions. Adenylate kinase is a small monomeric enzyme that catalyzes the reversible conversion of AMP and ATP into two ADP molecules. Previous structural studies have revealed that substrate binding is accompanied by large rate-limiting spatial displacements of both the ATP and AMP binding motifs. In this report a solution-state NMR approach was used to probe the native energy landscape of adenylate kinase in its free form, in complex with its natural substrates, and in the presence of a tight binding inhibitor. Binding of ATP induces a dynamic equilibrium in which the ATP binding motif populates both the open and the closed conformations with almost equal populations. A similar scenario is observed for AMP binding, which induces an equilibrium between open and closed conformations of the AMP binding motif. These ATP- and AMP-bound structural ensembles represent complexes that exist transiently during catalysis. Simultaneous binding of AMP and ATP is required to force both substrate binding motifs to close cooperatively. In addition, a previously unknown unidirectional energetic coupling between the ATP and AMP binding sites was discovered. On the basis of these and previous results, we propose that adenylate kinase belongs to a group of enzymes whose substrates act to shift pre-existing equilibria toward catalytically active states.

Introduction

Enzymes are efficient biocatalysts that can increase the rates of chemical reactions several orders of magnitude. Detailed understanding of the native energy landscape during catalysis is a prerequisite to comprehend how biocatalysts can lower transition-state energies. Enzymes may in their ligand-free states undergo intrinsic fluctuations that are related to the motions required for catalysis. For these enzymes, substrate binding in part serves to shift a pre-existing equilibrium toward catalytically potent states. This idea has been suggested for both RNase A[1] and cyclophilin A.[2] Advances in NMR spectroscopy have allowed unprecedented characterization of such fluctuations. Adenylate kinase (adk) is a small enzyme that catalyzes the reversible conversion of ATP and AMP into two ADP molecules (Scheme 1) and serves as an excellent model system to study the relationship between structure, dynamics, and enzymatic activity. Adk contains two substrate binding domains that undergo significant spatial translations upon substrate binding. In this paper, these domains are designated AMPbd and ATPlid. The crystal structures of adk isolated from *Escherichia coli* (Eadk) have been solved both in the open apo state to 2.2 Å resolution[3] and in complex with the tight binding inhibitor Ap5A

Scheme 1. Reaction Catalyzed by Adk

$$AMP + ATP \underset{Mg^{2+}}{\overset{Mg^{2+}}{\rightleftharpoons}} 2\,ADP$$

(P^1, P^5-di(adenosine-5′-)pentaphosphate) to 1.9 Å resolution.[4] Both the ATPlid and the AMPbd occupy closed conformations in the Ap5A-bound structure. Phosphoryl group transfer from ATP to AMP occurs in the closed, solvent excluded conformation. The magnitude of the conformational exchange during domain closure enables direct detection of this catalytically important process with NMR methods. Fluctuations of the substrate binding domains are rate-limiting for adk catalysis.[5] Through recent technical improvements, solution-state NMR has turned out to be extremely useful in the study of enzymes in their active states.[6−10] Here, we present a detailed solution-state NMR examination of the native energy landscape of Eadk in response to binding of Ap5A and its natural substrates AMP, ATP, and ADP. Binding of either AMP or ATP forces the individual substrate binding domains into equilibrium, with approximately equal numbers of molecules populating the open

(1) Beach, H.; Cole, R.; Gill, M. L.; Loria, J. P. *J. Am. Chem. Soc.* **2005**, *127*, 9167−9176.
(2) Eisenmesser, E. Z.; Millet, O.; Labeikovsky, W.; Korzhnev, D. M.; Wolf-Watz, M.; Bosco, D. A.; Skalicky, J. J.; Kay, L. E.; Kern, D. *Nature* **2005**, *438*, 117−121.
(3) Müller, C. W.; Schlauderer, G. J.; Reinstein, J.; Schulz, G. E. *Structure* **1996**, *4*, 147−156.
(4) Müller, C. W.; Schulz, G. E. *J. Mol. Biol.* **1992**, *224*, 159−177.
(5) Wolf-Watz, M.; Thai, V.; Henzler-Wildman, K.; Hadjipavlou, G.; Eisenmesser, E. Z.; Kern, D. *Nat. Struct. Mol. Biol.* **2004**, *11*, 945−949.
(6) Tollinger, M.; Skrynnikov, N. R.; Mulder, F. A.; Forman-Kay, J. D.; Kay, L. E. *J. Am. Chem. Soc.* **2001**, *123*, 11341−11352.
(7) Loria, J. P.; Rance, M.; Palmer, A. G. *J. Am. Chem. Soc.* **1999**, *121*, 2331−2332.
(8) Boehr, D. D.; Dyson, H. J.; Wright, P. E. *Chem. Rev.* **2006**, *106*, 3055−3079.
(9) Bax, A.; Kontaxis, G.; Tjandra, N. *Methods Enzymol.* **2001**, *339*, 127−174.
(10) Eisenmesser, E. Z.; Bosco, D. A.; Akke, M.; Kern, D. *Science* **2002**, *295*, 1520−1523.

and closed states simultaneously. These equilibrium structural ensembles represent complexes that are populated transiently during adk catalysis. Both substrates are required for the enzyme to close both binding domains in a cooperative manner. Inspection of both open and closed Eadk structures suggests that hydrogen bonds, at least in part, account for the observed cooperativity. A unidirectional coupling between the ATPlid and the AMPbd was discovered on the basis of the chemical-shift correlations and microscopic binding constants. The data presented here, together with other theoretical and experimental studies, suggest that adk belongs to a group of enzymes that undergo pre-existing fluctuations resembling the motions required for catalysis. The addition of natural substrates acts to shift the free-energy landscape toward the catalytically active closed state.

Results and Discussion

Residual Dipolar Couplings of Open and Closed States. A prerequisite to be able to probe the energy landscape of adk in response to binding of its natural substrates is a characterization of the solution conformations of the open and closed states. RDCs (residual dipolar couplings) are NMR interactions that provide global structural information that can be used to define relative domain orientations in proteins. In regular buffer, these interactions are averaged to zero because of the isotropic tumbling of most proteins. By using an anisotropic medium, RDCs can be introduced into solution-state NMR owing to partial alignment of proteins in the applied external magnetic field. Partial alignment can be achieved with a number of different media (for a review, see for example ref 11). There exist a number of cases in which RDCs have been used to define the relative domain orientations in multidomain proteins.[12−15] The approach used here was to measure amide proton-backbone nitrogen ($^1D_{NH}$) RDCs of different Eadk states with subsequent fitting of these data to the crystallographically determined open and closed states. Alignment was introduced using the method of stretched polyacrylamide gels.[16,17] All IPAP (inphase antiphase) ^1H -^{15}N HSQC (heteronuclear single quantum coherence) NMR spectra used for the quantification of RDCs are of high quality, with narrow linewidths showing no apparent sign of protein aggregation.

Ap5A is a tight binding inhibitor with a dissociation constant to adk of around 2.5 nM.[18] Accordingly the binding of Ap5A to Eadk is slow on the NMR time scale. The high binding affinity ensures that the completely saturated and closed state can be populated in the NMR tube. Thus, Ap5A-bound Eadk serves as a reference of the closed state. In addition, the crystallographic structure of Eadk in complex with Ap5A has been solved to 1.9 Å resolution,[4] providing a firm structural basis for interpretation of experimental results. The best fitted parameters of the RDC experiments are summarized in Table 1. Apo Eadk is best fitted to the crystallographic open state based on χ^2 values, rmsd, and the quality factor Q.[19] The relatively high Q factor (0.37) associated with the open state might be caused by fluctuations of the flexible ATPlid and AMPbd. Fluctuations will act to reduce the quality of the fit by introducing a distribution of alignment tensors. The quality of fits of individual subdomains in apo Eadk is presented in Table 2. It is evident that RDCs of amino acids located in the region that is invariant to conformational flexibility, that is, the core domain, are less affected owing to averaging than residues in the flexible AMPbd and ATPlid. Even in light of the Q value, the RDC data indicate that the major alignment tensor of apo Eadk originates from the open state. Hence, the solution structural ensemble of apo Eadk is in essence very similar to the crystallographic open state, implying that chemical shifts measured in this state primarily report on the open conformation. Ap5A-bound Eadk is, as expected, populating the closed state on the basis of the fit of RDC data. Bearing in mind that the fit was done directly to a crystallographic structure, the Q factor associated with the closed state is relatively small. Since the Ap5A-bound state is closed in solution, chemical shifts in this state can be used as molecular probes of the closed conformation. Eadk has residual activity in the absence of Mg^{2+}, which is the condition used in all experiments described here. Addition of ADP to Eadk will produce an equilibrium mixture of AMP, ATP, and ADP. The equilibrium constant for the reaction in Scheme 1 is close to one, based on integration of one-dimensional ^{31}P NMR experiments (data not shown). The ADP-bound species has the most well-defined positioning of the AMPbd and the ATPlid, with both firmly populating the closed conformation. The high quality of the fits, with a low Q factor (0.20), is consistent with a well-defined state that is accurately

Table 1. Parameters for Fitting of $^1D_{NH}$ RDCs to Eadk[a]

state	PDB file	Da (Hz)	R (Dr/Da)	χ^2	rmsd (Hz)	R^b	Q^c	n^d
apo	1AKE	5.80	0.66	1080	3.80	0.80	0.61	75
	4AKE	−8.05	0.51	399	2.31	0.93	0.37	75
Ap5A	1AKE	−5.42	0.26	186	1.47	0.96	0.28	86
	4AKE	−5.90	0.33	549	2.53	0.87	0.49	86
ADP	1AKE	−5.58	0.29	103	1.07	0.98	0.20	90
	4AKE	−5.63	0.39	657	2.70	0.86	0.50	90

[a] Only residues that are in regular secondary structure in both 1AKE.pdb and 4AKE.pdb were subjected to analysis. These residues are: 2−7, 13−24, 28, 29, 31−40, 50−54, 61−71, 81−84, 90−98, 105−110, 113−121, 123−126, 131−134, 161−174, 177−187, 192−197, and 202−213. [b] R value for linear fit of fitted versus observed RDC. [c] Quality Q-factor.[19] [d] Number of $^1D_{NH}$ RDCs used in the fits.

Table 2. Fits of $^1D_{NH}$ RDCs to Subdomains of apo Eadk[a]

subdomain[b]	rmsd (Hz)	χ^2	n^c
core domain	1.96	154	40
AMPbd	2.89	125	15
ATPlid	2.45	120	20

[a] The best fitted alignment tensor of apo to 4AKE from Table 1 was used to calculate RDCs [b] Only residues defined in Table 1 were analyzed with the AMPbd and ATPlid defined as residues 28−72 and 113−176, respectively. [c] Number of residues analyzed in each subdomain.

(11) Tolman, J. R.; Ruan, K. *Chem. Rev.* **2006**, *106*, 1720−1736.
(12) Fischer, M. W.; Losonczi, J. A.; Weaver, J. L.; Prestegard, J. H. *Biochemistry* **1999**, *38*, 9013−9022.
(13) Skrynnikov, N. R.; Goto, N. K.; Yang, D.; Choy, W. Y.; Tolman, J. R.; Mueller, G. A.; Kay, L. E. *J. Mol. Biol.* **2000**, *295*, 1265−1273.
(14) Tsui, V.; Zhu, L. M.; Huang, T. H.; Wright, P. E.; Case, D. A. *J. Biomol. NMR* **2000**, *16*, 9−21.
(15) Hofmann, G.; Schweimer, K.; Kiessling, A.; Hofinger, E.; Bauer, F.; Hoffmann, S.; Rösch, P.; Campbell, I. D.; Werner, J. M.; Sticht, H. *Biochemistry* **2005**, *44*, 13043−13050.
(16) Sass, H. J.; Musco, G.; Stahl, S. J.; Wingfield, P. T.; Grzesiek, S. *J. Biomol. NMR* **2000**, *18*, 303−309.
(17) Tycko, R.; Blanco, F. J.; Ishii, Y. *J. Am. Chem. Soc.* **2000**, *122*, 9340−9341.
(18) Lienhard, G. E.; Secemski, I. I. *J. Biol. Chem.* **1973**, *248*, 1121−1123.
(19) Cornilescu, G.; Marquardt, J. L.; Ottiger, M.; Bax, A. *J. Am. Chem. Soc.* **1998**, *120*, 6836−6837.

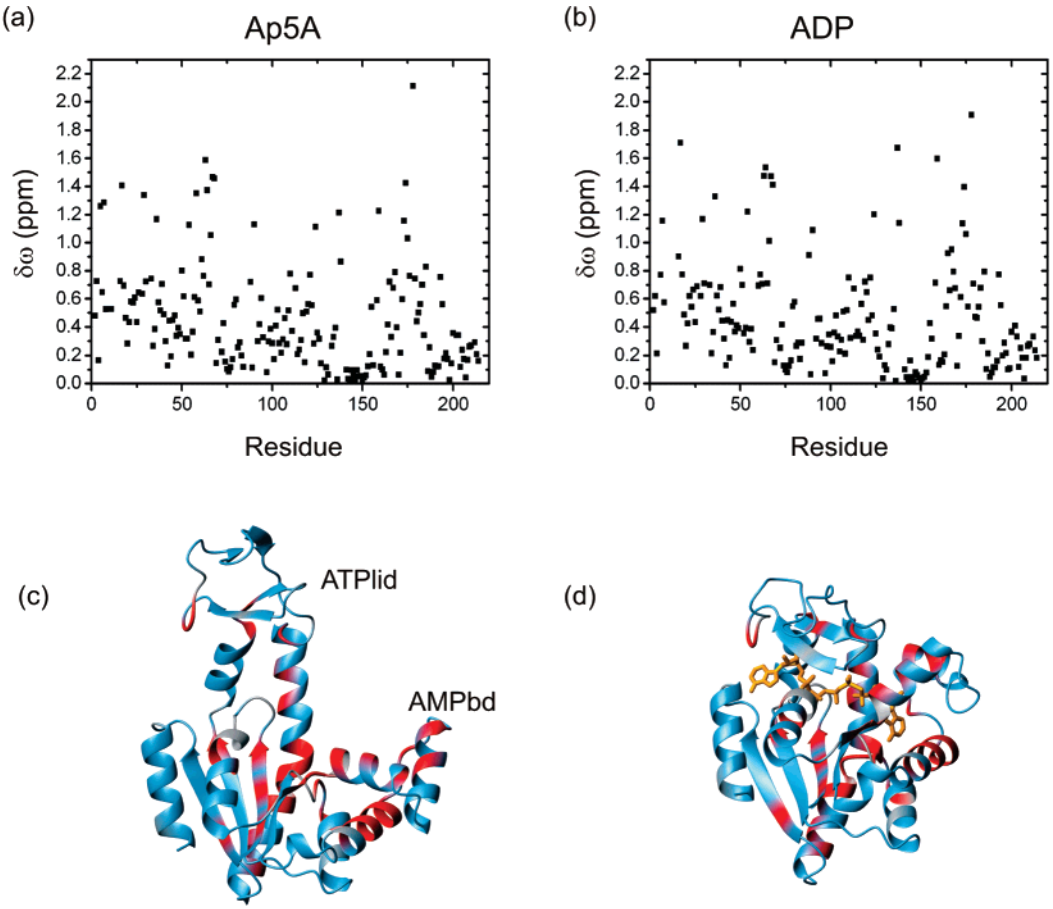

Figure 1. Chemical-shift perturbations of Eadk bound to Ap5A and ADP. All chemical shifts were measured with ^{1}H-^{15}N HSQC experiments of substrate-saturated samples at 25 °C with enzyme concentrations of 0.5 mM. Chemical-shift perturbations are relative to Eadk in the apo state and are calculated as the absolute value of a normalized sum of nitrogen and proton perturbations according to $\delta\omega = |0.2\Delta^{15}\mathrm{N} + \Delta^{1}\mathrm{H}|$ (ppm). (a, b) Chemical-shift perturbations plotted as a function of primary sequence. The Ap5A-bound state was obtained using 2.5 mM Ap5A (a), and the ADP-bound state was obtained in the presence of 20 mM ADP (b). (c, d) Spatial distribution of residues with chemical-shift perturbations in the Ap5A-saturated state larger than 0.7 ppm are colored red on the open (c) and closed (d) conformations of Eadk. Prolines and unassigned and overlapping residues are colored gray. The inhibitor is yellow and shown in a ball-and-stick representation. All protein figures in this paper were generated with the molecular graphics program MOLMOL.[21]

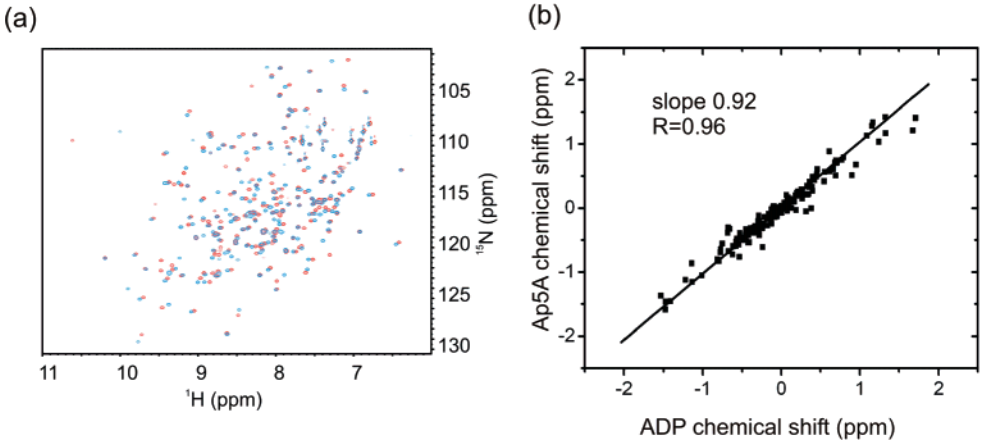

Figure 2. Chemical shifts show that ADP-bound Eadk in solution populates a closed conformation. (a) Superimposition of ^{1}H-^{15}N HSQC spectra of ADP-bound (red) and Ap5A-bound (blue) Eadk samples. (b) Correlation between chemical shifts in Ap5A- and ADP-saturated states of Eadk. Chemical-shift perturbations were calculated with respect to the apo state and are normalized according to $\delta\omega = 0.2\Delta^{15}\mathrm{N} + \Delta^{1}\mathrm{H}$ (ppm). The straight line represents a linear fit of Ap5A chemical shifts against ADP chemical shifts. The strong correlation and slope close to one show that the Ap5A- and ADP-bound states represent virtually identical three-dimensional solution structures.

described with one alignment tensor. The closed ADP-bound conformation is thus a well-defined structural state with limited conformational fluctuations as judged from the RDC measurements.

Fits of RDCs to the closed (1AKE.pdb) and open structures (4AKE.pdb) were performed using the program PALES.[20]

(20) Zweckstetter, M.; Bax, A. *J. Am. Chem. Soc.* **2000**, *122*, 3791−3792.

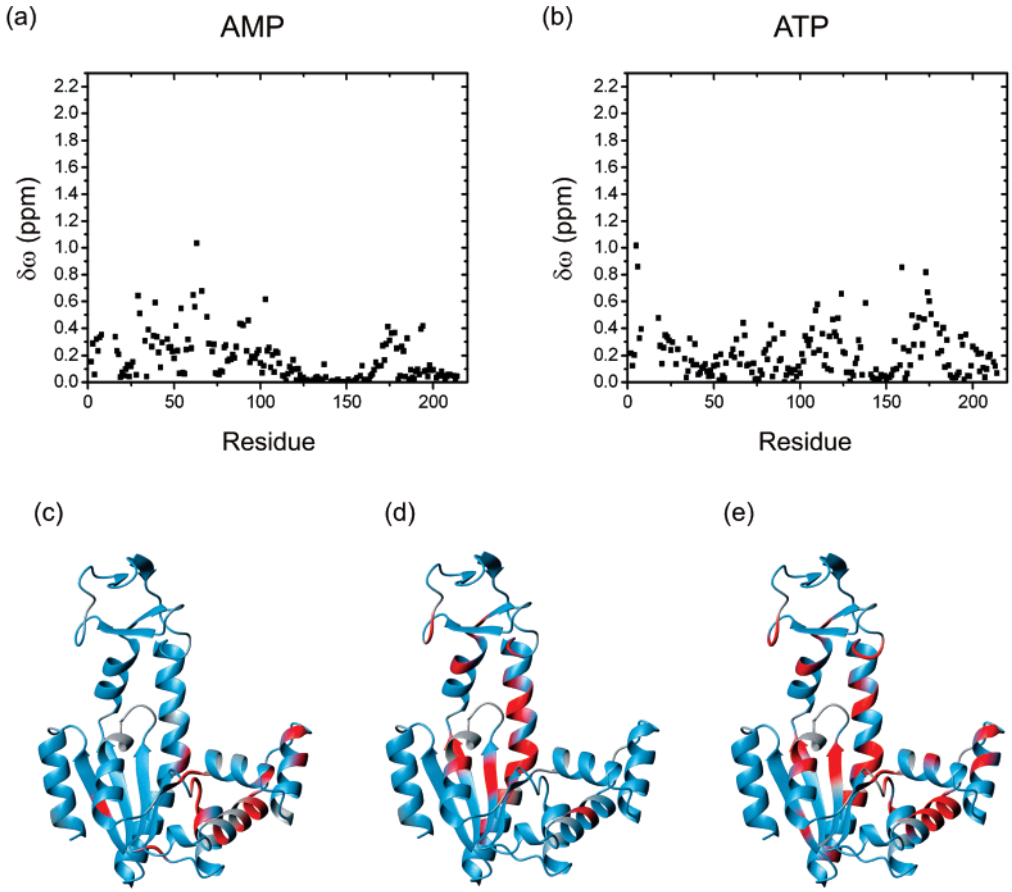

Figure 3. Chemical-shift perturbations of Eadk bound to AMP or ATP: (a) chemical-shift perturbations of Eadk saturated with AMP, plotted as function of the primary sequence; (b) perturbations of Eadk saturated with ATP, displayed against the primary sequence. Chemical-shift perturbations were calculated as in Figure 1. (c−e) Spatial distribution of chemical-shift perturbations plotted on the open Eadk structure: AMP-saturated state (c); ATP-saturated state (d). The ADP-saturated state is included as a reference for the distribution of shift perturbations (e). The threshold values for the AMP- and ATP-bound states were set to 0.4 ppm, whereas the threshold in the ADP-bound state was set to 0.7 ppm. Residues with chemical-shift perturbations larger than the threshold values are colored red. Unassigned, overlapping, and proline residues are colored gray.

Solution Conformation of ADP-Bound Eadk from Chemical Shifts. To address whether chemical shifts can be used to independently show that the ADP-bound state does indeed populate the crystallographically closed conformation in solution, chemical-shift perturbations between the Ap5A-bound and ADP-bound states were compared (Figure 1A,B). The spatial distribution of chemical-shift perturbations in the Ap5A-bound state is illustrated on the open and closed structures in Figure 1C and D. Both nucleotide binding motifs show extensive chemical-shift perturbations and harbor a large number of residues that can be used as reporters of the closed state. In Figure 2A, the ^{1}H-^{15}N HSQC spectra of the ADP- and Ap5A-bound states are superimposed. The spectra are similar to each other, suggesting that they originate from Eadk populating related three-dimensional structures. A plot of the chemical shifts in the two states against each other (Figure 2B) yields an excellent linear correlation with a slope close to unity (0.92) and an *R* value of 0.96. The strong correlation between the chemical shifts shows unambiguously that the ADP-bound state in solution is structurally very similar to the crystallographically closed state, and that the additional phosphate group present in Ap5A does not contribute significantly to the observed chemical-shift perturbations. Since both substrate binding domains are closed in the ADP-bound state, for the rest of this paper this state will be considered a reference of the closed conformation. The rationale is to avoid any possible discrep-

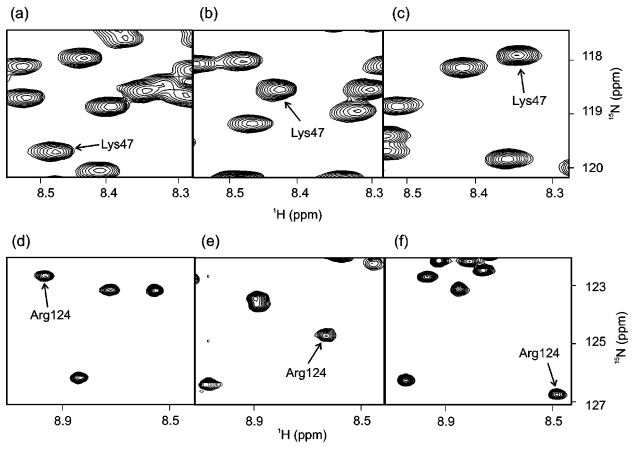

Figure 4. Chemical shifts of Lys47 and Arg124 in nucleotide-bound states suggest population averaging. (a−c) Expansions of ^{1}H-^{15}N HSQC spectra of Lys47 located in the AMPbd domain in the apo (a), AMP-saturated (b), and ADP-saturated states (c). The chemical shifts of Lys47 in the AMP-bound state are positioned between the chemical shifts of the apo and ADP states. (d−f) Expansions of ^{1}H-^{15}N HSQC spectra of Arg124 located in the ATPlid in the apo (d), ATP-saturated (e), and ADP-saturated states (f). The chemical shifts of Arg124 in the ATP state appear to fall on a straight line in-between the chemical shifts of the apo and ADP states. The NMR spectra were acquired at 25 °C with 20 mM of the respective substrate present.

(21) Koradi, R.; Billeter, M.; Wuthrich, K. *J. Mol. Graph.* **1996**, *14*, 51−55, 29−32.

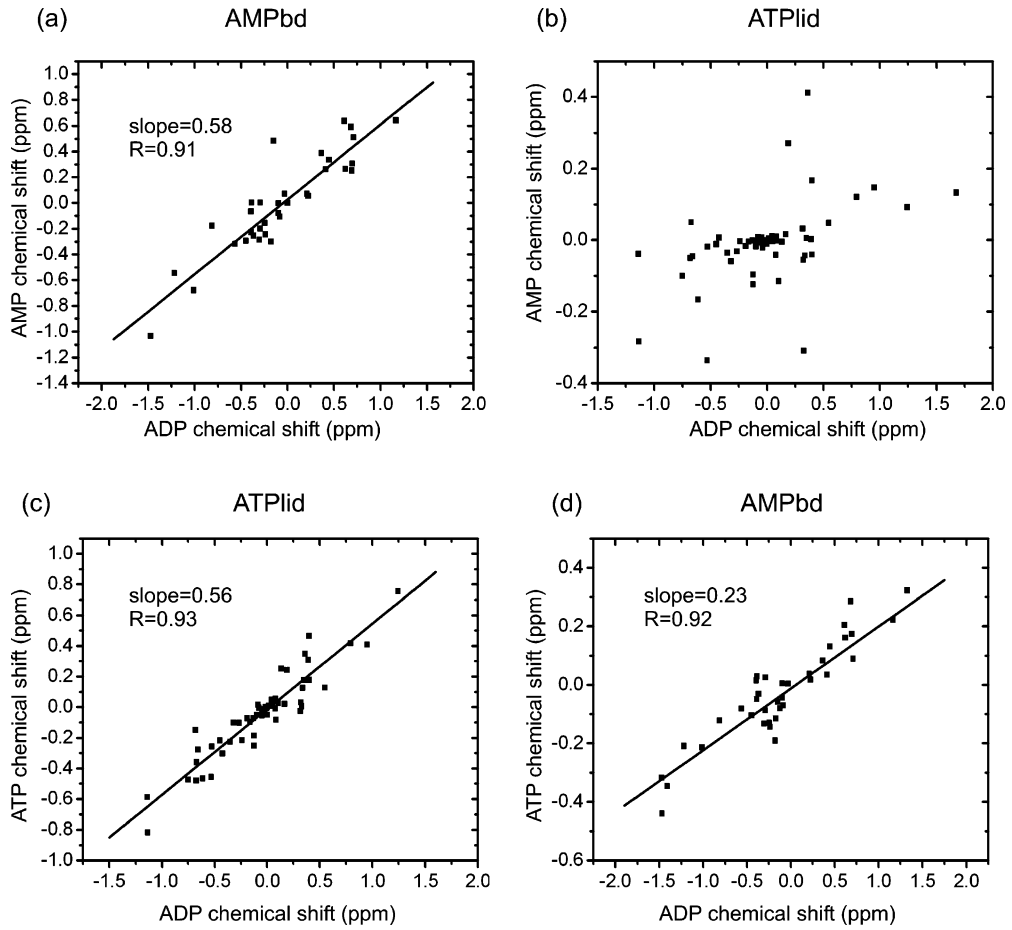

Figure 5. Global correlation between chemical-shift perturbations in AMP-, ATP-, and ADP-bound states. The domain boundaries were defined as residues 28−72 for the AMPbd and 113−176 for the ATPlid. Linear fits of the data are shown as lines in each section. Chemical-shift perturbations were calculated as in Figure 2: (a) correlation between AMP and ADP chemical shifts for the AMPbd. (b) correlation between AMP- and ADP-induced chemical shifts for the ATPlid. Due to the lack of correlation between the chemical shifts, no linear fit was performed; (c) correlation between ATP- and ADP-induced chemical shifts for the ATPlid; (d) correlation between ATP- and ADP-induced chemical shifts for the AMPbd.

ancies introduced by using the unnatural compound Ap5A as reference. The large chemical-shift differences induced by Ap5A binding and the resemblance between the ADP and Ap5A-bound states are quantified in Supporting Information Figure S1 and Table S1.

Chemical Shifts in AMP- and ATP-Bound States. With a reliable natural reference of the closed state in solution the structural response to AMP and ATP binding can be analyzed using chemical-shift perturbations (Figure 3A,B). Chemical shifts in substrate saturated states were measured relative to apo Eadk. Overall, the magnitude of the chemical-shift perturbations proved to be much smaller in both the AMP- and ATP-bound states than in the ADP-bound state, but were found to be localized mainly to the respective binding sites (Figure 3C,D). The reduced amplitude is unexpected in the ATP complex, since ATP binding has been suggested to stimulate complete closure of the ATPlid. This suggestion has been inferred from the crystallographic structure of yeast adk in complex with the nonhydrolyzable ATP analogue $AMPPCF_2P$.[22] Complete closure of the ATPlid would introduce perturbations that overall have similar amplitude as the ones observed in the closed ADP-bound state. On the basis of the reduced chemical shifts it is obvious that neither the ATPlid nor the AMPbd is completely closed in the singly nucleotide-bound states.

Domain Closure from Chemical Shifts. It is possible to extract detailed quantitative information on the process of domain closure from chemical-shift perturbation analysis. This is crucial in order to identify the mechanism behind the reduced chemical shifts in the AMP- and ATP-bound states. Visual inspection of NMR spectra in apo, AMP-, and ADP-bound states reveals that the chemical shifts of residues in the AMPbd appear to be correlated between these states. In Figure 4A−C this observation is shown for Lys47, which is located in the AMPbd. The chemical shifts of Lys47 in the AMP-bound state appear to fall on a straight line between the chemical shifts of the apo and the ADP-bound states. A similar scenario is observed for residues in the ATPlid when NMR spectra in the apo, the ATP-bound, and the ADP-bound states are inspected. This observation is shown for Arg124 located in the ATPlid in Figure 4D-F. The correlations suggest that the chemical shifts of the single nucleotide-bound states contain contributions from both apo- and ADP-bound states.

The presence of partial shifts toward the ADP-bound conformation in the single nucleotide-bound states for Lys47 and Arg124 warranted a global quantification of these observations. In the following analysis the AMPbd and ATPlid were treated

(22) Schlauderer, G. J.; Proba, K.; Schulz, G. E. *J. Mol. Biol.* **1996**, *256*, 223−227.

Table 3. Apparent Dissociation Constants of ATP and AMP to Wild-Type Eadk and the R88A Mutant

protein	nucleotide	domain	K_D [μM]	n^a
wild type	AMP	AMPbd	210 ± 66	39
		ATPlid	1700 ± 400	6
	ATP	AMPbd	53 ± 74	14
		ATPlid	50 ± 31	34
R88A	AMP	AMPbd	8500 ± 2000	26
		ATPlid	4800 ± 850	9
	ATP	AMPbd	36 ± 30	5
		ATPlid	98 ± 40	33

[a] Number of probes (^{1}H or ^{15}N chemical shifts) used for fitting of binding constants and their associated experimental uncertainties. Only non-overlapping resonances with an absolute chemical-shift change exceeding 54 Hz in the ^{1}H dimension or 36 Hz in the ^{15}N dimension were subjected to analysis.

separately. In Figure 5, the chemical-shift perturbations that resulted from AMP or ATP binding are plotted against the ADP-bound chemical shifts. Virtually all residues in the AMPbd displayed chemical shifts that fell onto a straight line when AMP- and ADP-bound states were compared (Figure 5A). The data can be fitted accurately to a straight line with a slope equal to 0.58. The simplest explanation for this observation is that the chemical shifts of residues in the AMPbd are population-weighted averages in the AMP-bound state. Since all chemical-shift perturbations are calculated relative to apo Eadk, the averaged chemical shifts are composed of one term from the apo state and one term from the ADP-bound state. The apo- and ADP-bound states in solution are well described with the crystallographic determined open and closed states as shown with RDCs and chemical shifts, suggesting that the averaging in the AMPbd occurs between open and closed conformations:

$$\omega^{obs} = p^{apo}\omega^{apo} + p^{closed}\omega^{closed} \quad (1)$$

where ω^{obs} is the observed chemical shift, ω^{apo} and ω^{closed} are chemical shifts of the apo- and ADP-bound states, and p^{apo} and p^{closed} are populations of these states. The chemical shifts of the apo state mainly report on the crystallographically open conformation, but are also expected to be affected by fluctuations in this state. Chemical shifts in the ADP-bound state are likewise reporters, primarily of the closed state, but as shown previously[5] the closed state is in equilibrium with the open conformation. Equation 1 is valid under the condition of fast exchange which is confirmed for the binding events addressed in this study.

We conclude that residues in the AMPbd are involved in a dynamic equilibrium with populations of the open and closed conformations being equal to 58% and 42%, respectively. This dynamic equilibrium represents a transient AMP-bound structural ensemble that is an integral part of Eadk catalysis. In contrast to the strong correlation observed for residues in the AMPbd, AMP binding is not correlated to ADP binding for residues in the ATPlid (Figure 5B). The small perturbations present in the ATPlid are likely a result of unspecific binding of AMP, a conclusion that is strengthened further by the analysis of dissociation constants given below.

Quantification of perturbations induced by ATP binding reveal a strong global correlation for residues in the ATPlid with the chemical shifts observed in the ADP-bound state. A linear fit resulted in a slope of 0.56 (Figure 5C). Using the same

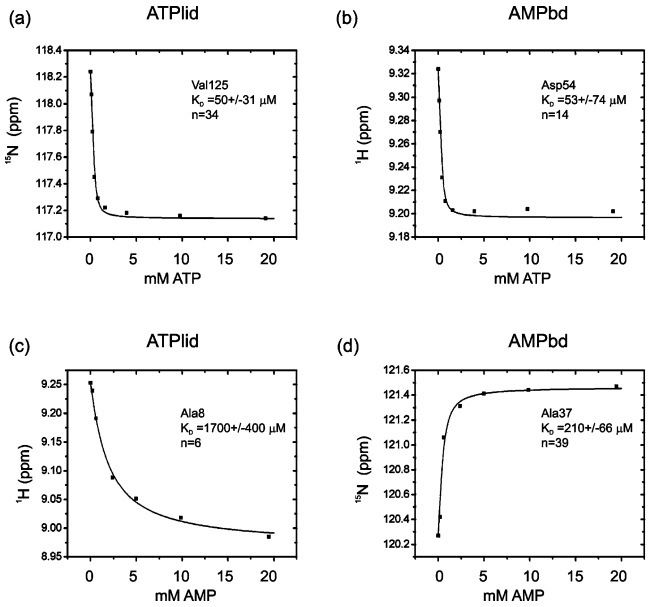

Figure 6. Apparent dissociation constants of ATP and AMP to wild-type Eadk. K_D values for residues sensitive to AMP or ATP binding were quantified by fitting the observed chemical-shift changes in ^{1}H-^{15}N HSQC experiments as a function of added substrate to eq 2. Domain boundaries are defined in Figure S2 and Table S2. ^{1}H and ^{15}N chemical shifts were treated independently. Only residues with an absolute chemical-shift change exceeding 54 Hz in the ^{1}H dimension or 36 Hz in the ^{15}N dimension were subjected to analysis: (a, b) K_D values for ATP binding to the ATPlid (a) and the AMPbd (b); (c, d) K_D values for AMP binding to the ATPlid (c) and the AMPbd (d).

argument as above, we suggest that this correlation is a result of chemical-shift averaging between the open and closed states. The ATP-bound state is thus also a transient structural ensemble, where the ATPlid interconvert between open and closed states. It is interesting to note that AMPPCF$_2$P-bound[22] yeast adk was crystallized with the ATPlid positioned in the closed conformation. These data are fully consistent with our model, bearing in mind that only stable configurations can crystallize; hence, the AMPPCF$_2$P-yeast adk complex is likely trapped in a state where the ATPlid is fully closed.

Notably, ATP binding induces perturbations in the AMPbd which is located far away from the ATPlid in the three-dimensional structure. These chemical-shift perturbations do not originate from unspecific binding of ATP to the AMPbd, which is discussed further below. Chemical-shift correlations were analyzed using the method described above, and there exist a strong linear dependence between chemical shifts in the ATP- and ADP-bound states for residues in the AMPbd (Figure 5D). The best-fitted straight line has a slope of 0.23. Perturbation of the ATPlid by ATP binding apparently affects residues in the AMPbd in a global manner. This observation is consistent with the existence of an intramolecular communication pathway spanning from the ATPlid to the AMPbd. A structural model that accounts for the observed energetic coupling is that residues in the AMPbd are forced into equilibrium between open and closed conformations in response to ATP binding. This equilibrium is only partially shifted toward the closed state with the fraction of molecules in the closed state approximately equal to 0.23.

Intramolecular Coupling Probed with Microscopic Dissociation Constants. Solution-state NMR provides the unique possibility to quantify dissociation constants with residue-

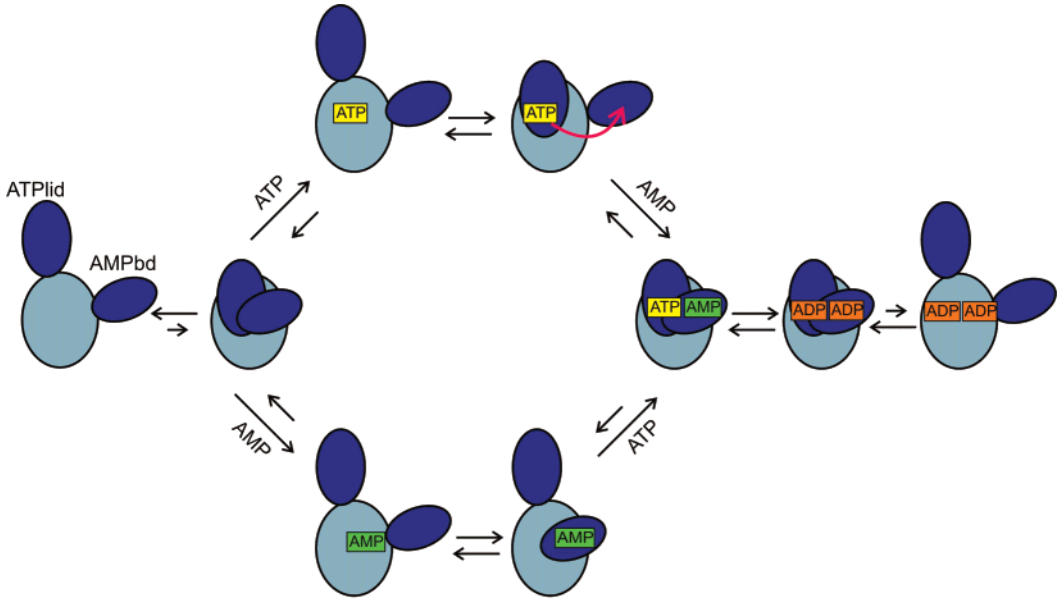

Figure 7. Domain movement and equilibria during Eadk catalysis. The scheme is based on a random bi−bi mechanism that has been proposed for adk[24] and has been expanded according to the findings in this paper together with previous results. (Left) The apo Eadk appears to be involved in a pre-existing equilibrium where the ATPlid and the AMPbd samples the closed conformations. (Top) Binding of ATP introduces an interconversion between open and closed states for residues in the ATPlid with an equilibrium constant close to one. ATP binding is also energetically coupled to the AMPbd as indicated with the red arrow. (Bottom) AMP binding introduces an equilibrium in the AMPbd between open and closed states with an equilibrium constant approximately equal to one. Binding of correct substrates to both the ATPlid and the AMPbd will make the binding motifs to close cooperatively. (Right) The bound state with either one AMP and one ATP molecule or two ADP molecules bound is in equilibrium between open and closed states.[5] The degree of closure of the nucleotide binding motifs increases from left to right in the figure.

specific resolution. The spatial distribution of K_D values is a complementary approach to study the coupling between the ATPlid and AMPbd that was suggested from chemical-shift perturbations. Binding constants were quantified by monitoring observed chemical-shift perturbations as a function of increasing AMP or ATP concentration. The data were subsequently fitted to a two-state binding model according to

$$\omega^{obs} = \omega^{apo} + (\omega^{bound} - \omega^{apo})\left[\frac{K_A(E_{tot} + L_{tot}) + 1}{2K_A E_{tot}} - \sqrt{\left(\frac{K_A(E_{tot} + L_{tot}) + 1}{2K_A E_{tot}}\right)^2 - \frac{L_{tot}}{E_{tot}}}\right] \quad (2)$$

where ω^{obs} is the observed chemical shift, ω^{bound} is the chemical shift of the bound conformation, ω^{apo} is the chemical shift of the apo state, K_A is the association constant, E_{tot} is the total enzyme concentration, and L_{tot} is the total ligand concentration. Fitted parameters are K_A and ω^{bound}.

Both ATP and AMP binding are in fast exchange on the chemical-shift time scale, since resonances move progressively from the apo state toward the bound states as functions of nucleotide concentration. K_D values were analyzed in the context of the domain boundaries identified in Figure S2 and Table S2. The results are summarized in Table 3. Representative binding isotherms with the best-fitted binding curves are shown in Figure 6. ATP binds to the ATPlid with a K_D value of 50 ± 31 μM. Interestingly, residues in the AMPbd report on a process with a very similar K_D value (53 ± 74 μM). The overlap between the distributions of observed binding constants in both the ATPlid and AMPbd is consistent with coupling between the ATP and AMP binding sites. Perturbation of the ATPlid by means of ATP binding will thus induce a concerted structural response at the AMPbd. AMP binds to the AMPbd with a K_D value of 210 ± 66 μM. On the other hand, the ATPlid shows very weak AMP binding, and the fitted K_D value is 1700 ± 400 μM. This result supports our interpretation that AMP binds nonspecifically to the ATP binding site. Unspecific AMP binding has previously been suggested to explain the observed AMP-mediated inhibition of adk at high AMP concentrations.[23] Our data provide further evidence to support this conclusion. On the basis of the magnitude of the K_D values observed, there is no evidence for communication in the direction from the AMPbd to the ATPlid. Hence, the coupling appears to span unidirectionally from the ATPlid to the AMPbd. It is important to point out that the communication suggested is not an effect of unspecific binding of ATP to the AMPbd. Two experiments were performed to rule out this possibility. First, the enzymatic activity of Eadk was measured using a coupled spectroscopic assay[24] as a function of ATP concentration. There was no sign of ATP inhibition even at ATP concentrations of 2 mM (data not shown). Given the observed K_D value for ATP at the AMPbd (53 ± 74 μM), inhibition would have been expected for direct binding. Second, we quantified residue-specific K_D values for an Arg88Ala mutation (Table 3). The X-ray structure of Ap5A-bound Eadk indicates that position 88 is crucial for AMP binding. This has also been shown experimentally with an Arg88Gly mutation, which leads to an 85-fold increase in the apparent K_M for AMP and a reduction of the catalytic activity to less than 1% compared to the wild type.[25] Mutation of this position basically removes AMP binding, which is the boundary condition required for the NMR experiment. As expected, the

(23) Sinev, M. A.; Sineva, E. V.; Ittah, V.; Haas, E. *FEBS Lett.* **1996**, *397*, 273−276.
(24) Rhoads, D. G.; Lowenstein, J. M. *J. Biol. Chem.* **1968**, *243*, 3963−3972.
(25) Reinstein, J.; Gilles, A. M.; Rose, T.; Wittinghofer, A.; Saint Girons, I.; Bârzu, O.; Surewicz, W. K.; Mantsch, H. H. *J. Biol. Chem.* **1989**, *264*, 8107−8112.

mutation dramatically reduces the affinity of Eadk for AMP; the K_D value increases to 8.5 ± 2 mM for the AMPbd and to 4.8 ± 0.85 mM for the ATPlid. The magnitude of the K_D values shows that the AMP binding site is effectively removed. Binding of ATP is, however, not significantly perturbed in the mutant enzyme. ATP binds to the ATPlid with a K_D value of 98 ± 40 μM, which is within the experimental error compared to the K_D observed for the wild-type enzyme. Even with the AMP site removed, we observed a K_D value at the AMPbd of 36 ± 30 μM. This binding is apparently not due to unspecific binding of ATP. The overlap between the distributions of observed K_D values at the ATPlid and AMPbd in response to ATP is preserved in the mutated enzyme. The binding constants observed in wild-type and mutant Eadk constitutes further strong support for the existence of a unidirectional communication pathway in the direction from the ATPlid to the AMPbd.

Conclusions.

We have analyzed the native energy landscape of Eadk in response to binding of its natural substrates AMP, ATP, and ADP and the tight binding inhibitor Ap5A using solution state NMR methods. The data presented here, together with previously published experiments, allow us to propose a detailed structural model for adk catalysis (Figure 7). Both experimental and theoretical work suggests that the ATPlid and AMPbd is highly flexible in the apo state. In a study of intermolecular distances between Val169 (located in the ATPlid) and Ala55 (located in the AMPbd) of Eadk using time-resolved energy transfer measurements, the apo enzyme displayed a broad distance distribution[26] with mean and width of 31 and 29 Å, respectively. This result is consistent with large scale fluctuations of the substrate binding motifs in the ligand-free state. A recent computer simulation of apo adk[27] suggested that the ATPlid and AMPbd fluctuate between the open state and conformations that are similar to the closed crystallographic Ap5A-bound state. Our RDC measurements of apo Eadk are also consistent with a highly flexible enzyme that adopts a distribution of alignment tensors owing to fluctuations of the nucleotide binding domains. Finally, the fact that Eadk populates the open conformation with almost 50% occupancy in the AMP- and ATP-bound states indicates that the enzyme must have the innate ability to interconvert between open and closed conformations. Taken together, these observations can be rationalized with a model in which Eadk, in its ligand-free state, fluctuates between the open and closed conformations with the major population in the open state.

The central part of Figure 7 relates to the identification of transient structural ensembles. In contrast to the traditional view of ligand binding where bound complexes are structurally well defined, both the ATP- and the AMP-bound states are structural ensembles that populate open and closed conformations in equilibrium. A detailed structural view of these dynamic equilibria is shown in Figure 8. The equilibrium constant of these interconversions are close to one; hence, the free energies of open and closed states are virtually identical in these transient complexes. The addition of AMP or ATP will act to increase the lifetime of the closed state by stabilizing the system with

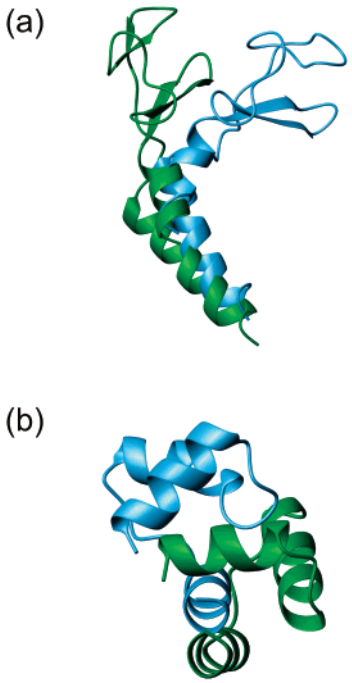

Figure 8. Structural representation of the transient complexes populated during Eadk catalysis. (a) ATP binding is illustrated with the conformations of the ATPlid in the crystallographic open (green) and closed (blue) conformations. These conformations represent the equilibrium shown in the top of Figure 7. (b) Structural states for residues in the AMPbd in response to AMP binding illustrated using the same color coding as in panel a. This equilibrium corresponds to the bottom part of Figure 7.

favorable interactions. The AMP- and ATP-bound states are true transient states since binding of the second substrate will force both binding domains to close cooperatively. The binding of ATP to the ATPlid is in addition energetically coupled to the AMPbd. We suggest that the output of this coupling is an equilibrium between the open and closed states in the AMPbd.

At least part of the energetic basis underlying the cooperativity of domain closure can be identified in the crystallographic structure of Ap5A-bound Eadk (Figure 9A and B) and is mediated through both protein−substrate and protein−protein hydrogen bonds. Arginine 156 positioned at the top of the ATPlid donates hydrogen bonds to both the γ-phosphate of the ATP moiety and the α-phosphate of the AMP moiety in one of the two molecules of the asymmetric unit as pointed out in ref 4. A protein−protein hydrogen bond is formed between the backbone amide proton of Leu58 in the AMPbd, and a carboxyl oxygen in the side chain of Glu170, located in the ATPlid. These three hydrogen bonds can only be formed when both binding domains are closed simultaneously and couples the AMPbd and the ATPlid energetically. Opening and closing of the substrate binding sites with both ATP and AMP present is thus a correlated event based on the hydrogen-bonding pattern and the results presented here. This inference is in line with the observation that the substrate binding lids fluctuate with equal rates during catalytic turnover.[5] It has been shown using relaxation dispersion measurements that the ADP-bound state exists in equilibrium between the open and closed conformations (right part of Figure 7). This equilibrium is skewed toward the closed state, and reopening of the ATPlid and the AMPbd is rate limiting for catalysis.[5] In summary, going from left to right in Figure 7, the degree of closure of the substrate binding lids

(26) Sinev, M. A.; Sineva, E. V.; Ittah, V.; Haas, E. *Biochemistry* **1996**, *35*, 6425−6437.
(27) Lou, H. F.; Cukier, R. I. *J. Phys. Chem. B* **2006**, *110*, 24121−24137.

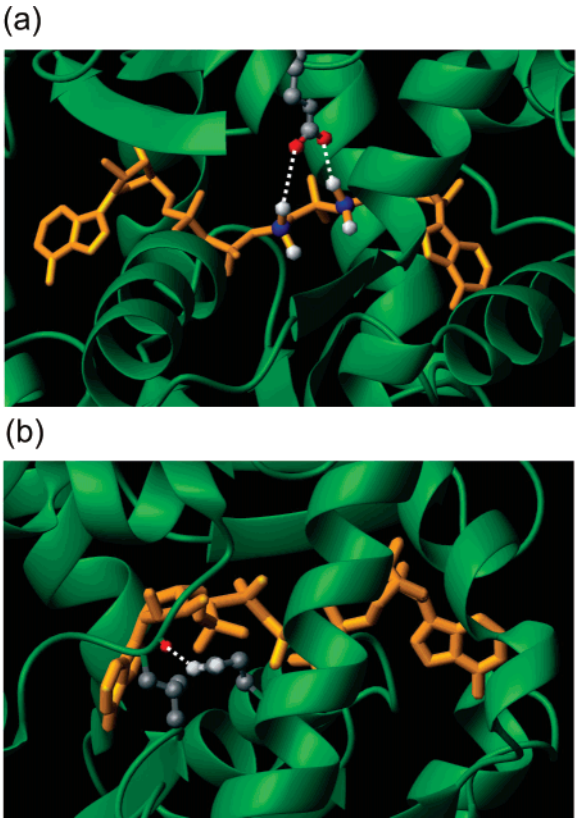

Figure 9. Structural basis for cooperative domain closure in Eadk. Hydrogen bonds that only can form with both the ATPlid and the AMPbd closed are shown as white dotted lines on the X-ray structure of Ap5A (yellow)-bound Eadk. (a) Hydrogen bonds between side-chain protons of Arg156 (red) and oxygens (white) attached to phosphates corresponding to the γ-phosphate of ATP (left) and the α-phosphate of AMP (right). (b) Hydrogen bond donated from the backbone amide proton of Leu58 (red) in the AMPbd to a side-chain carboxyl oxygen of Glu170 (white) in the ATPlid. The view has been rotated almost 180° with respect to that shown in panel a.

is gradually increased as a function of occupancy of the correct nucleotide at the respective binding sites.

A new view of enzymatic catalysis is currently emerging, primarily from NMR observations. It has been suggested that cyclophilin A possesses innate fluctuations that are conserved between the resting and catalytically active states.[2] Binding of substrate acts to shift a pre-existing equilibrium toward the catalytically active state where the chemistry can occur. Similar conclusions have been drawn from an NMR study of RNase A in free and inhibitor-bound states.[1] This new concept has been strengthened in a recent report on the dynamics of dihydrofolate reductase.[28] It was shown that dihydrofolate reductase can populate high-energy states in preceding intermediates along the reaction trajectory. The addition of substrates serves to shift pre-existing equilibria toward the next step in the catalytic cycle. The data presented here suggest that adenylate kinase belongs to this exciting group of enzymes. The transient ATP- and AMP-bound ensembles indicate that Eadk has the innate ability to populate the catalytically active closed conformation; subsequent binding of substrates will gradually shift the enzyme toward the fully closed state. These new ideas add additional constraints to the evolution of enzymes. Enzymes have not only evolved flexible active sites that can accommodate ligands, transfer functional groups, and lower transition-state energies, these active sites have evolved to be flexible with the innate ability to make excursions to exited states that have "ligand-bound-like" structure.

(28) Boehr, D. D.; McElheny, D.; Dyson, H. J.; Wright, P. E. *Science* **2006**, *313*, 1638−1642.

Materials and Methods

Site-Specific Mutagenesis. Site-directed mutagenesis was performed using the Quick Change method (Stratagene). Correct insertion of the Arg88Ala mutation was confirmed with DNA sequencing (MWG Biotech).

Protein Preparation and NMR Spectroscopy. Eadk was prepared as outlined in ref 5. The NMR samples contained 0.5−1.0 mM ^{15}N-labeled or ^{15}N, ^{13}C-labeled protein with 2 mM TCEP, 50 mM NaCl, and 30 mM MOPS at pH 7.0 with 10% (v/v) $^{2}H_2O$. All NMR experiments were acquired at 25 °C on a Bruker DRX 600 MHz spectrometer equipped with a 5-mm triple resonance *z*-gradient cryoprobe. Data were processed using the NMRPipe software[29] and visualized using ANSIG for Windows.[30] Backbone resonance assignments of Eadk in the apo form were carried out previously.[5] Eadk in the Ap5A-complexed state was assigned using the triple-resonance experiments HNCAB[31] and CBCA(CO)NH[32] together with a ^{15}N NOESY-HSQC experiment. Eadk in complex with AMP, ATP, and ADP was assigned on the basis of the combination of ^{15}N NOESY-HSQC and substrate titration experiments. Substrate titrations were performed using AMP, ATP, ADP, and Ap5A purchased from Sigma-Aldrich. Partial alignment was introduced with strained-induced alignment in polyacrylamide gels.[16,17] Enzyme-containing polyacrylamide gels were stretched using the apparatus described in ref 33 (New Era Enterprises). Gels were cast in Teflon cylinders of 5 mm inner diameter and subsequently transferred into open-ended NMR tubes (New Era Enterprises) with an inner diameter of 4.2 mm. All gels were prepared from a stock solution containing 29.2% w/v acrylamide and 0.78% *N*,*N*′-methylenebisacrylamide. The required amount of acrylamide−bisacrylamide stock solution was diluted to a final concentration of 4.75%. Ammonium persulfate (0.09% w/v) and 0.8% TEMED were added to intiate polymerization. The gel was allowed to polymerize overnight and was washed extensively afterward with the NMR buffer. An appropriate length of the gel cylinder was transferred into a tube that contained 350 μL of Eadk at concentrations ranging from 1.5 to 1.9 mM. For substrate-containing samples AMP, ATP, ADP, or Ap5A was present at the appropriate concentration. Enzyme and substrate were allowed to diffuse into the acrylamide gel for at least 12 h prior to transfer into NMR tubes. $^{1}D_{NH}$ residual dipolar couplings were measured using the IPAP ^{1}H -^{15}N HSQC pulse sequence.[34] Reference samples were prepared using the appropriate substrate concentrations in the NMR buffer.

Binding constants were quantified by fitting the chemical-shift perturbations in ^{1}H -^{15}N HSQC experiments as a function of stepwise addition of substrate to eq 2. Global binding constants were calculated as being the average of the K_D values measured for individual nuclei. The error was estimated from the standard deviation of the sampled K_D values.

Acknowledgment. This work was supported financially by the Swedish Research Council. Dr. Tobias Sparrman is acknowledged for maintaining the NMR facility.

(29) Delaglio, F.; Grzesiek, S.; Vuister, G. W.; Zhu, G.; Pfeifer, J.; Bax, A. *J. Biomol. NMR* **1995**, *6*, 277−293.
(30) Helgstrand, M.; Kraulis, P.; Allard, P.; Härd, T. *J. Biomol. NMR* **2000**, *18*, 329−336.
(31) Wittekind, M.; Mueller, L. *J. Magn. Res. Series B* **1993**, *101*, 201−205.
(32) Grzesiek, S.; Bax, A. *J. Am. Chem. Soc.* **1992**, *114*, 6291−6293.
(33) Chou, J. J.; Gaemers, S.; Howder, B.; Louis, J. M.; Bax, A. *J. Biomol. NMR* **2001**, *21*, 377−382.
(34) Ottiger, M.; Delaglio, F.; Bax, A. *J. Magn. Reson.* **1998**, *131*, 373−378.

Supporting Information Available: Figure S1 and Table S1: Quantification of chemical-shift differences between Ap5A-bound and apo or ADP-bound Eadk. Figure S2 and Table S2: Chemical-shift-based identification of the spatial distribution of residues sensitive to AMP or ATP binding. This material is available free of charge via the Internet at http://pubs.acs.org.

JA075055G